Kinetics of Oxygen Surface Exchange on Epitaxial Ruddlesden-Popper Phases and Correlations to First-Principles Descriptors

Yueh-Lin Lee[1‡], Dongkyu Lee[1,2‡], Xiao Renshaw Wang[1], Ho Nyung Lee[2], Dane Morgan[3] and Yang Shao-Horn[1,*]*

[1]*Electrochemical Energy Laboratory, Massachusetts Institute of Technology, 77 Massachusetts Avenue, Cambridge, Massachusetts 02139, United States*

[2]*Materials Science and Technology Division, Oak Ridge National Laboratory, Oak Ridge, Tennessee 37831, United States*

[3]*Department of Materials Science and Engineering, University of Wisconsin–Madison, Madison, Wisconsin 53706, USA*

* Corresponding Authors

* Email: ddmorgan@wisc.edu; shaohorn@mit.edu

Author Contributions

‡These authors contributed equally.

ABSTRACT.

Through alignment of theoretical modeling with experimental measurements of oxygen surface exchange kinetics on (001)-oriented $La_{2-x}Sr_xMO_{4+\delta}$ (M= Co, Ni, Cu) thin films, we demonstrate, here, the capability of the theoretical bulk O *2p*-band centers to correlate with oxygen surface exchange kinetics of the Ruddlesden-Popper oxide (RP_{214}) (001)-oriented thin films. In addition, we demonstrate that the bulk O *2p*-band centers can also correlate with the experimental activation energies for bulk oxygen transport and oxygen surface exchange of both the RP_{214} and the perovskite polycrystalline materials reported in the literature, indicating effectiveness of the bulk O *2p*-band centers in describing the associated energetics and kinetics. We propose that the opposite slopes of the bulk O *2p*-band center correlations between the RP_{214} and the perovskite materials is due to the intrinsic mechanistic differences of their oxygen surface exchange kinetics bulk anionic transport.

TOC GRAPHICS

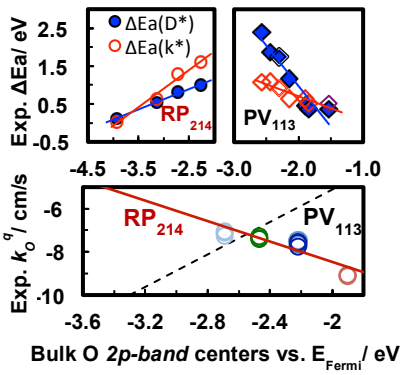

Bulk O 2p band centers and k_O^q data for perovskites (PV_{113}) reproduced from Ref. 33 © 2011 with permission from the Royal Society of Chemistry

Ruddlesden-Popper (RP) oxides such as $A_{2-x}A'_xMO_{4+\delta}$ (A=La, Pr, Nd; A'=Ca, Sr, Ba; M= Co, Ni, Cu) are promising alternative cathode materials for intermediate temperature (between 500~700 °C) solid oxide fuel cells (IT-SOFC).[1-4] In contrast to perovskites where oxygen vacancies are generally the dominant anion defect, these RP_{214} oxides can switch between hypostoichiometric and hyperstoichiometric regimes, where the oxygen off-stoichiometry comes from their majority oxygen defects.[5-6] Consequently, oxygen diffusion in the RP_{214} phases can potentially occur *via* mechanisms associated with either oxygen interstitials or oxygen vacancies, or both. Recent neutron scattering studies[7] and molecular dynamic simulations[8-10] indicate that oxygen diffusion in the hyperstoichiometric RP_{214} phases involves spontaneous migration of oxygen interstitials along with their neighboring apical oxygens from the rocksalt layers. Such an oxygen interstitialcy (push-pull) diffusion mechanism takes place anisotropically in the RP_{214} structure, leading to significantly different oxygen ion transport along different orientations.[11-12] For example, the kinetics of oxygen transport parallel to the *a-b* planes in the $A_2NiO_{4+\delta}$ is considerably higher than that of the out-of-plane direction, by up to two orders of magnitude.[12] Strong coupling to lattice dynamics is further proposed to play a critical role in the oxygen transport in the RP_{214} phases at ambient/moderate temperatures, where presence of oxygen interstitial in the A_2O_2 rocksalt layers significantly activates A-site-atom and apical-O displacements along [110] directions, resulting in enhancement in the oxygen interstitialcy migration through phonon-assisted diffusion.[13-14] Although the origin of the phonon-assisted diffusion is different from the classical push–pull mechanism activated at higher temperatures, both oxygen transport mechanisms are coupled to, or mediated by, oxygen interstitials in the undoped RP_{214} phases.[13, 15] Similar to the oxygen diffusion properties, anisotropic oxygen surface exchange kinetics was also reported for the RP_{214} materials, where the in-plane surface exchange

kinetics can be about five times greater than that of the out-of-plane for $A_2NiO_{4+\delta}$ single crystals,[11, 14] and the enhancement was shown to be even greater (up to two orders of magnitude) in epitaxial thin films.[12]

Substitution of aliovalent cations such as Sr^{2+} or Ba^{2+} for La^{3+} in La-based RP_{214} phases can also dramatically influence the anisotropy in the oxygen transport and surface exchange kinetics. In particular, an enhancement on electronic conductivity can be obtained *via* aliovalent cation substitution and in contrast to the SOFC perovskites, the overall effect upon increasing Sr^{2+} or Ba^{2+} content to a high doping level in general leads to reduction of the oxygen diffusion coefficients.[5, 16-19] Recently, we have reported that increase of Sr^{2+} doping content can lead to a change in the $La_{2-x}Sr_xNiO_{4\pm\delta}$ ($0 \le x \le 1.0$) film orientation from the (100) to the (001) direction, which is accompanied by reduction in the oxygen surface exchange coefficients (k_O^q) by two orders of magnitude based on electrochemical impedance spectroscopy (EIS) measurements.[20] Density functional theory (DFT) calculations further revealed that Sr^{2+} substitution can greatly weaken adsorption of molecular oxygen as well as stabilize the (001) surface relative to the (100) surface.[20] These results indicate a potential convolution between Sr^{2+} doping level and change of relative surface stability of (100) termination *vs*. (001) termination of the $La_{2-x}Sr_xNiO_{4\pm\delta}$ thin films, both of which can result in reduction of oxygen surface exchange kinetics. Very recently, Chen *et al*.[21] reported that Sr^{2+} concentration in the epitaxially grown $La_{2-x}Sr_xCoO_{4\pm\delta}$ thin films exhibits greater influence on their surface exchange kinetics than the orientation, which is attributed to reduction of oxygen interstitial capacity of the $La_{2-x}Sr_xCoO_{4\pm\delta}$ upon increasing the Sr^{2+} doping level, thereby making incorporation of oxygen from the surfaces to the lattice more difficult. Similar observation in oxygen vacancy dominated RP phases was also recently reported for $(La,Sr)_{n+1}(Co,Fe)_nO_{3n+1-\delta}$ at different n (n=1, 2, and 3).[22] The outer surfaces of

$(La,Sr)_{n+1}(Co,Fe)_nO_{3n+1-\delta}$ were shown to exhibit similar chemical composition whereas their oxygen surface exchange kinetics are varied by 1~2 orders of magnitude. Tomkiewicz *et al.*[22] conclude that there exists a significant contribution of "bulk" transport rates within the measurement of the surface exchange rates, resulting in the empirical k_O *vs.* D_O correlations. Overall, these results indicate that despite structural similarity, much greater complexity occurs in the RP_{214} systems than the perovskite materials, due to coupling and interplay between material anisotropy, bulk defect chemistry, and lattice dynamics, which have either direct or indirect influences on their bulk oxygen transport and oxygen surface exchange kinetics. Therefore it is of significant interest to assess and distinguish how these intrinsic properties influence the surface exchange and oxygen reduction kinetics of the RP_{214} phases for SOFC cathode applications.

As a first step toward understanding and predicting the complex behavior of the RP_{214} materials associated with their oxygen surface exchange kinetics, in this work we demonstrate significant simplification of the many attributes that influence surface exchange to a small number of underlying factors, through systematic investigation of oxygen surface exchange kinetics for a series of (001)-oriented RP_{214} thin films. While the anisotropy effect may lead to distinct oxygen mobility and surface exchange rate for the RP_{214} phases, the k_O^q values extracted from a series of (001)-oriented RP_{214} films provides data for constrained material systems where influences from material anisotropy are minimized, which allows one to reduce variables and elucidate the influence of intrinsic material factors.

The (001)-oriented oriented epitaxial $La_{2-x}Sr_xMO_{4\pm\delta}$ (x = 0, 0.15, 0.4, 1 and M = Cu, Co, Ni) thin films on a $(001)_{cubic}$-yttria-stabilized -zirconia (YSZ) substrate with a gadolinia-doped-ceria (GDC, with 20 mol% Gd) as the buffer layer were deposited using pulsed laser deposition

(PLD), as shown in Figure 1(a). Normal X-ray diffraction (XRD) data of all films, details of deposition on XRD, lattice parameters, and AFM images of the films are further provided in the Supporting Information (Figure S1~S3, and Table S1). The surface exchange kinetics was examined using EIS measurements conducted on patterned microelectrodes (~200 μm) fabricated by photolithography and acid etching[23]. Representative EIS data collected from the $La_{2-x}Sr_xMO_{4\pm\delta}$ films at 550 °C with an oxygen partial pressure ($p(O)_2$) of 0.1 atm are shown in Figure 1(b), where all films exhibit nearly perfect predominant semicircle impedances. Considering the fact that all film thicknesses are much smaller than the critical thickness for bulk transport limitation (estimated to be ~3, ~87 and ~ 5000 μm for the bulk La_2CuO_4[24], La_2NiO_4[25], and La_2CoO_4[26], respectively), the ORR kinetics are limited by surface oxygen exchange but not by oxygen ion diffusion.[27-28] The dominant role of surface exchange is further supported by the observed $p(O_2)$-dependent impedance responses expected for a surface oxygen exchange kinetics limited electrode,[29-30] as shown in Figure S4, Supporting Information. The k_O^q values of all films grown with the *c*-axis perpendicular to the film surface are shown in Figure 1(c). The $p(O_2)$ dependence of k_O^q (k_O^q α $p(O_2)^m$) was found to be in the range from 0.59 to 0.89 of all the investigated $La_{2-x}Sr_xMO_{4\pm\delta}$ (Figure 1(c)), indicating the reaction rate-limiting step is a molecular oxygen absorption dissociation process rather than a charge transfer process.[31-32]

By controlling orientation of the epitaxial thin films and integrating with theoretical modeling, we demonstrate that the electronic structure descriptor of SOFC perovskites – the bulk O *2p*-band center[33] – also correlates with the surface exchange kinetics of the (001)-oriented RP_{214} thin films, as well as the reported experimental activation energies of D_O^* and k_O^* of both the RP_{214} and the perovskite materials in the literature. While caution is needed to make a direct comparison between theoretically modeled surfaces and the real surfaces under the operating

conditions, as surface structures can reconstruct or surface chemical composition can deviate from the bulk (such as changing the A-site and B-site ratio or having Sr^{2+} segregation or enrichment on the surfaces[21, 34]), these ideal surface models provide a theoretical platform to extract important energetics and to explore trends of various materials, which have already been shown to be valuable in developing fundamental understanding across various material systems[33, 35] and surface terminations.[20, 36-37] Upon establishment of correlations between the bulk O *2p*-band centers and those of the simulated surfaces as well as the bulk/surface oxygen energetics across various RP_{214} materials, we then utilize its robustness to assess trends between the theoretical bulk O *2p*-band centers and experimentally measured kinetics of oxygen surface exchange and bulk oxygen diffusion, including both the rates and activation barriers, which underpin the bulk O *2p*-band center as a fundamental factor that govern surface catalytic activities of the complex oxides.

Figure 2 shows the computed O *2p*-band centers (relative to the Fermi level) of the top (001) AO surface layer, the second (001) BO_2 surface layer, and the averaged top two surface layers *vs*. those of the stoichiometric bulk RP_{214} phases (La_2NiO_4, La_2CuO_4, $LaSrCoO_4$, $La_{1.5}Sr_{0.5}CuO_4$, and $LaSrNiO_4$), and they all exhibit good linear correlations. These almost identical slopes of the correlations indicate that the averaged bulk O *2p*-band centers correlate with, and can be used to describe, the surface O *2p*-band centers. To the extent which O *2p*-band centers describe the physics of the local material this result suggests we can use bulk O *2p*-band centers to describe surface properties within similar surface structures and terminations. This result is further supported by the correlations between the surface/bulk oxygen energetics and the computed bulk O *2p*-band centers, as shown in Figure S8, Supporting Information.

By utilizing the capability of the bulk O *2p*-band centers to consistently describe surface electronic structures and oxygen defect energetics in the bulk and on the surface across various RP_{214} materials, we can assess trends associated with kinetics of oxygen surface exchange and bulk oxygen diffusion of the RP_{214} materials. A comparison between experimentally obtained k_O^q from our EIS measurements at T=550 °C and $p(O_2)$=1 atm and our calculated bulk O *2p*-band centers of the RP_{214} phases is performed and discussed below. As shown in Figure 3, our results reveal a good correlation exists between the experimentally measured surface exchange k_O^q for the (001) oriented epitaxial $La_{2-x}Sr_xMO_4$ (M=Co, Ni, and Cu) films in this work and their computed bulk O *2p*-band centers. In addition, the slope of the correlation was found to be negative while the slope of the surface exchange k_O^*/k_O^q *vs*. O *2p*-band center reported previously for the perovskite materials was positive[33]. The opposite k_O^*/k_O^q *vs*. the O *2p*-band slopes between the RP_{214} phases and the perovskite materials may be attributed to their distinct oxygen surface exchange and bulk oxygen transport mechanisms under the SOFC operating conditions. Specifically, we expect oxygen kinetics to be directly or indirectly mediated by oxygen interstitial related mechanisms in the RP_{214} materials and oxygen vacancy mediated mechanisms in the perovskites.

An attempt was made to extend the correlation observed in Figure 3 between the calculated bulk O *2p*-band centers and the k_O^q/k_O^* values of the RP_{214} materials under a similar operating condition from the literature (Figure S9, Supporting Information). Unfortunately, the large scattering of the data reported in the literature even for a single system such as $La_2NiO_{4+\delta}$[38] did not provide a clear statistical trend, in part due to the convoluted material properties and chemistry which impair reproducible experimental results for a direct comparison between different measurements on the same system synthesized/fabricated through different routes.

Therefore, we instead look into the reported activation barriers of bulk oxygen transport and oxygen surface exchange in the literature[5, 26, 38] *vs*. the computed bulk O *2p*-band centers, as we believe these energetic quantities might be more reproducible between different studies. In addition, these experimental activation energies are expected to be more directly associated with the bulk electronic structure descriptor of the RP_{214} phases than the total D_O* and k_O* values, which may couple to intrinsic materials properties such as orientation, microstructure, and small changes in defect concentrations. The experimentally extracted activation barriers of D_O* and k_O* of the polycrystalline RP_{214} reported in the literature[5, 26, 38] *vs.* the computed bulk O *2p*-band centers are shown in Figure 4(a), in which a good linear correlation is observed. The emergence of such correlations indicates the RP_{214} bulk O *2p*-band centers indeed govern the kinetics of D_O* and k_O*, and further suggests the need for improved data quality for experimental D_O* and k_O* of various bulk RP_{214} systems to establish such relationships. The same analysis was also performed on the SOFC perovskite materials, and the overall results are shown in Figure 4(b), where good linear correlations are also observed between the calculated bulk O *2p*-band centers *vs*. the activation barriers of D_O* and k_O* of the perovskite materials, except that the activation barrier of k_O* of $Ba_{0.5}Sr_{0.5}Co_{0.8}Fe_{0.2}O_{3-\delta}$, adopted in Ref. 2 is found to be an outlier of the correlation. Interestingly, the slopes of the activation barriers *vs*. bulk O *2p*-band correlations of the RP_{214} and the perovskite materials are again opposite (as in Figure 3), supporting the distinct mechanisms of oxygen surface exchange and bulk oxygen transport between the two different material systems. Overall, our results demonstrate the effectiveness of the electronic structure descriptor – the bulk O *2p*-band centers – in describing surface exchange and oxygen diffusion rates through the correlations to not only the key energetics of the bulk oxygen transport and surface exchange kinetics, but also the experimentally extracted activation barriers. Our results

suggest search and design of the active RP_{214} phases with direct or indirect oxygen interstitial mediated mechanisms should seek for good surface exchange and bulk transport in the materials with lower bulk O *2p*-band centers relative to the Fermi level, in contrast to the active SOFC perovskite materials, where the higher surface-exchange-coefficient materials have the higher O *2p*-band centers relative to the Fermi level.[33]

In summary, although significantly greater complexity exists in the RP_{214} phases than the perovskite materials due to the coupling among material anisotropy, oxygen defect chemistry, and lattice dynamics, by aligning the epitaxial thin films with DFT modeling on the bulk and surfaces, trends were revealed between the bulk electronic structure descriptor, the O *2p*-band center, and the experimentally measured k_O^qs of the (001)-oriented RP_{214} epitaxial thin films. Such a correlation between the experimental k_O^qs *vs*. the computed bulk O *2p*-band centers of the investigated RP_{214} materials is different from that obtained in the perovskite systems due to their opposite slopes, which are likely associated with their distinct active oxygen defects for bulk oxygen transport and surface exchange kinetics (oxygen interstitials for the RP_{214} phases and oxygen vacancies for the perovskites). In fact, these opposite slopes can be taken as strong support for the dominant role of interstitial over vacancy mediated kinetics in the RP_{214} materials. In addition, the bulk O *2p*-band centers further capture trends in the activation energies of bulk oxygen transport and surface oxygen exchange coefficients of both the RP_{214} and perovskite phases reported in the literature, supporting the effectiveness of the bulk O *2p*-band centers in describing the associated kinetics. On the other hand, the already close to zero activation energies extracted from the experimental Arrhenius plots for bulk oxygen transport and oxygen surface exchange of $La_2CoO_{4+\delta}$ indicate a potential material instability issue for search and development of active RP_{214} materials with the bulk O *2p*-band centers lower than that of

$La_2CoO_{4+\delta}$. Our combined theoretical and experimental study on well-defined surfaces of the RP_{214} phases underpins the bulk O *2p*-band center as a key fundamental material factor that governs surface catalytic activities of complex oxides. However, efforts are still needed to obtain detailed mechanistic understanding, including the role of factors such as material anisotropy, lattice dynamics *etc*., for the oxygen kinetics of the RP_{214} phases. Such understandings, combined with the O *2p*-band center descriptor, offer exciting opportunities for targeted search and development of RP_{214} materials for SOFC cathodes.

ABBREVIATIONS

RP, Ruddlesden-Popper; IT-SOFC, intermediate temperature solid oxide fuel cells; ORR, oxygen reduction reactions; PLD, Pulsed laser deposition; YSZ, Y_2O_3-stabilized ZrO_2; GDC, gadolinium-doped ceria; DFT, Density Functional Theory; EIS, electrochemical impedance spectroscopy;

NOTES

The authors declare no competing financial interests.

ACKNOWLEDGMENT

D. Morgan and Y.-L. Lee were supported by the Department of Energy (DOE), National Energy Technology Laboratory (NETL), Solid State Energy Conversion Alliance (SECA) Core Technology Program (Funding Opportunity Number DEFE0009435). D. Lee, X.R. Wang, and Y. Shao-Horn were supported by the Skoltech-MIT Center for Electrochemical Energy. Sample synthesis and structural characterization were performed at the Center for Nanophase Materials Sciences (CNMS), which is sponsored at Oak Ridge National Laboratory (ORNL) by the

Scientific User Facilities Division, Basic Energy Sciences (BES), U.S. DOE, and were also in part supported by the U.S. DOE, Office of Science, BES, Materials Sciences and Engineering Division (H. N. L.). Computational work was also benefited from the use of the National Energy Research Scientific Computing Center (NERSC) allocation of the CNMS at ORNL, both under grant number CNMS2013-292.

Supporting Information Available

Details about experimental methods, including sample preparation, EIS testing, and XRD, DFT modeling approaches, correlation between the bulk O *2p-and* surface O defect energetics, discussions on surface exchange and oxygen diffusion along the (001) orientation, and discussions on material instability of the RP_{214} phases *vs.* the perovskite materials are provided in electronic Supporting Information (SI†).

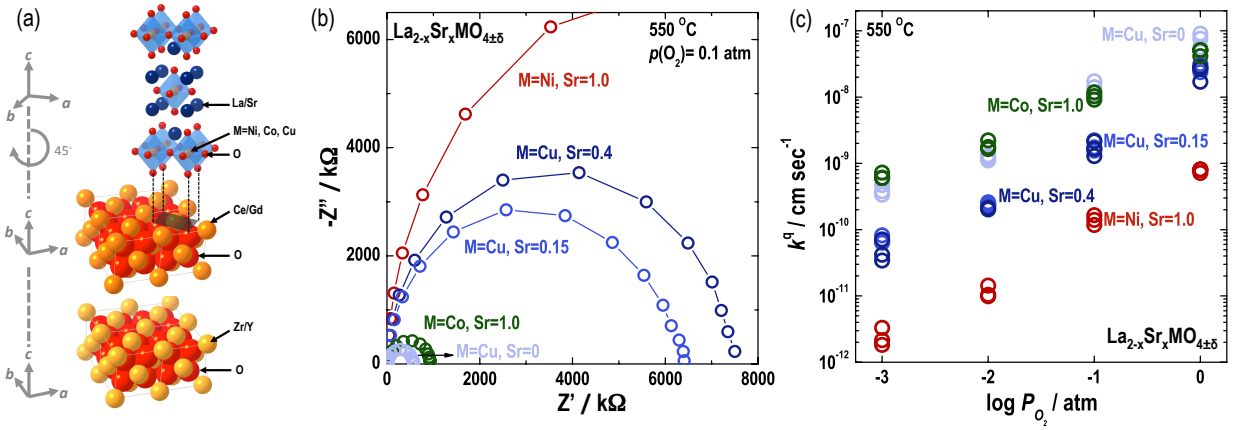

Figure 1. (a) Schematic of a *c*-axis oriented Ruddlesden-Popper (RP) oxide thin films epitaxially grown on a YSZ (001) substrate with a GDC buffer layer. (b) Nyquist plot and (c) oxygen partial pressure dependency of the surface exchange coefficients of $La_2CuO_{4+\delta}$ (light blue), $LaSrCoO_{4\pm\delta}$, (green), $La_{1.85}Sr_{0.4}CuO_{4\pm\delta}$ (blue), $La_{1.6}Sr_{0.4}CuO_{4\pm\delta}$ (deep blue) and $LaSrNiO_{4\pm\delta}$ (red) thin films calculated from EIS spectra collected at 550 °C. Three microelectrodes from each sample were measured at the same oxygen partial pressure. The *m* values of $La_2CuO_{4+\delta}$, $LaSrCoO_{4\pm\delta}$, $La_{1.6}Sr_{0.4}CuO_{4\pm\delta}$, $La_{1.85}Sr_{0.15}CuO_{4\pm\delta}$, and $LaSrNiO_{4\pm\delta}$ epitaxial thin films were approximately 0.79, 0.59, 0.86, 0.89 and 0.86, respectively.

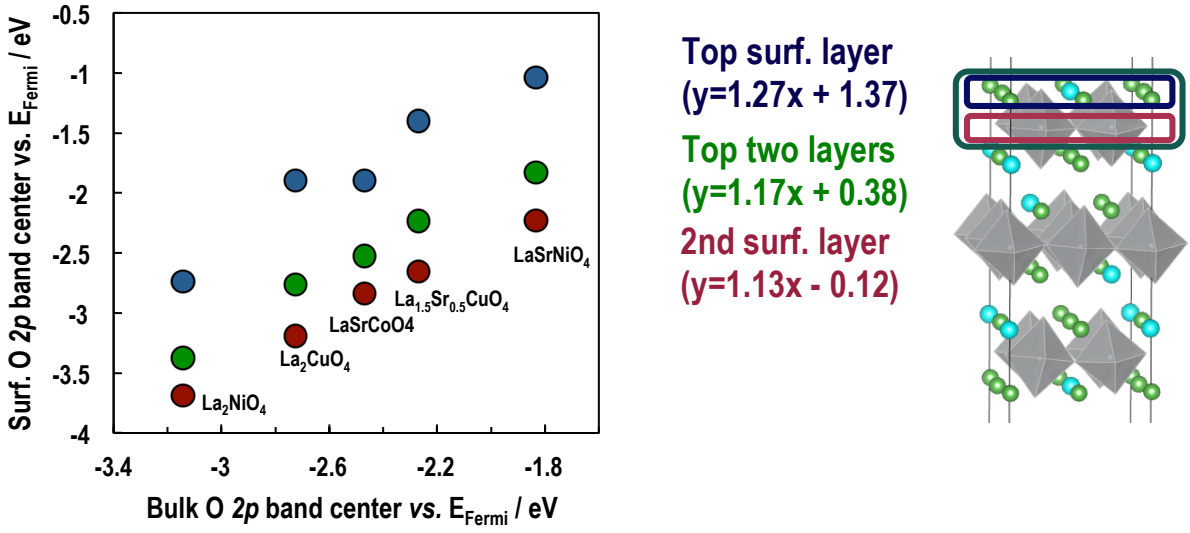

Figure 2. The computed DFT surface O *2p*-band centers (relative to the Fermi level, E_{Fermi}) of the top surface layer (blue), the second surface layer (red), and the top two surface layers (green) *vs.* the bulk O *2p*-band centers for La_2NiO_4, La_2CuO_4, $LaSrCoO_4$, $La_{1.5}Sr_{0.5}CuO_4$ and $LaSrNiO_4$. The slopes of the correlation are provided in the legend and a schematic of the (001) slab of the simulated $La_{2-x}Sr_xMO_4$ (La: green circles, Sr: blue circles and M-O octahedra: grey) is also provided on the right-hand-side of the figure. The empty rectangles highlight the surface layers where the O *2p*-band centers were computed.

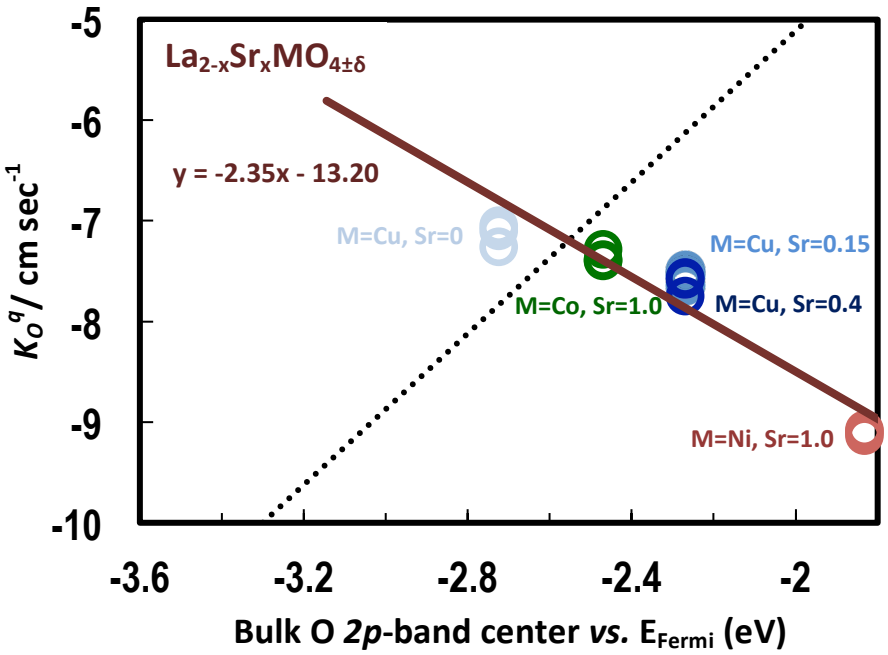

Figure 3. The oxygen surface exchange coefficients obtained from the EIS results of La_2CuO_4 (light blue), $LaSrCoO_4$ (green), $La_{1.85}Sr_{0.15}CuO_4$ (blue), $La_{1.6}Sr_{0.4}CuO_4$ (deep blue) and $LaSrNiO_4$ (red) films with (001) orientations measured at 550 ^{O}C *vs*. the computed DFT bulk O *2p*-band centers (relative to the Fermi level, E_{Fermi}). Due to the coarser composition grid of the DFT model, the bulk O *2p*-band centers of $La_{1.75}Sr_{0.25}CuO_4$, $La_{1.5}Sr_{0.5}CuO_4$ and $La_{1.75}Sr_{0.25}NiO_4$ were used for representing the k_O^q's of $La_{1.85}Sr_{0.15}CuO_4$, $La_{1.6}Sr_{0.4}CuO_4$ and $La_{1.8}Sr_{0.2}NiO_4$ in the figure. The grey dashed lines represents the correlation between experimental oxygen surface exchange coefficients and the computed bulk O *2p*-band centers for a series of SOFC perovskites,[33] reproduced from Ref. 33 © 2011 with permission from the Royal Society of Chemistry.

(a)

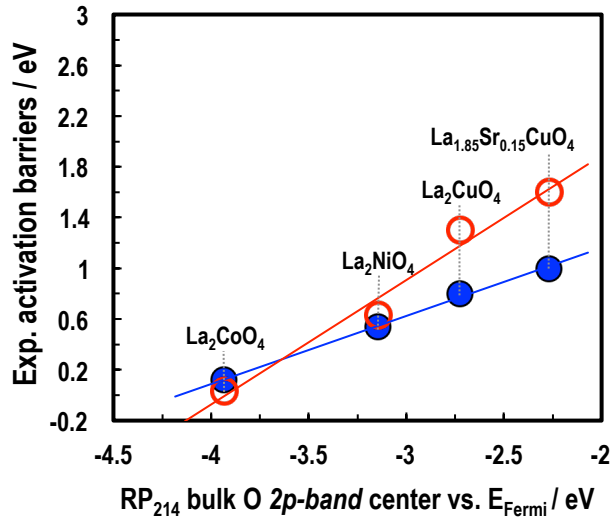

(b)

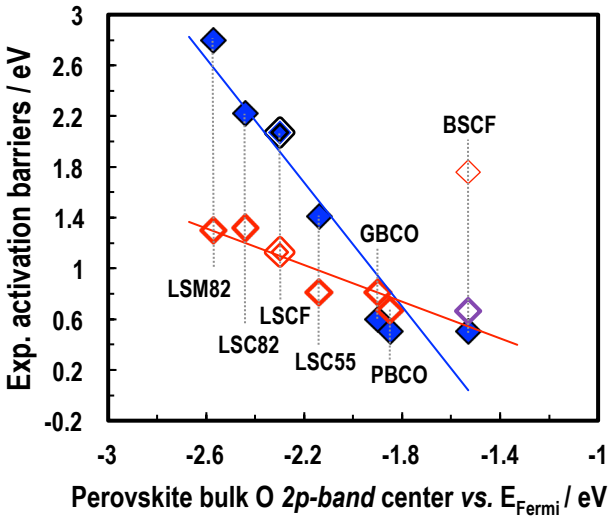

Figure 4. (a) The activation barriers (ΔE_a) for bulk oxygen transport (D_O*, blue filled circles) and oxygen surface exchange (k_O*, red empty circles) for $La_2CoO_{4+\delta}$,[26] $La_2NiO_{4+\delta}$,[38] $La_2CuO_{4+\delta}$,[5] and $La_{1.85}Sr_{0.15}CuO_{4+\delta}$,[5] *vs*. the computed bulk O *2p*-band centers; (b) the activation barriers (ΔE_a) for D_O* (blue filled diamonds) and k_O* (red empty diamonds) summarized in Table 1 of Ref. 2 for $La_{0.8}Sr_{0.2}MnO_{3+\delta}$ (LSM82), $La_{0.8}Sr_{0.2}CoO_{3-\delta}$ (LSC82), $La_{0.5}Sr_{0.5}CoO_{3+\delta}$ (LSC55), $GdBaCo_2O_{6-\delta}$ (GBCO), $PrBaCo_2O_{6-\delta}$ (PBCO), and $Ba_{0.5}Sr_{0.5}Co_{0.8}Fe_{0.2}O_{3-\delta}$ (BSCF) *vs*. the computed bulk O *2p*-band centers collected from the previous works[33, 39] (LSC55 from Ref. 39). For $La_{0.6}Sr_{0.4}Co_{0.2}Fe_{0.8}O_{3-\delta}$, both activation barriers of k_O* and D_O* (symbols with double lines) were taken from Ref. 40 instead of Ref. 2 (where the measurements were performed with GDC electrolyte instead of YSZ). Furthermore, additional data of the activation barrier of the BSCF surface exchange coefficients from Ref. 41 (empty purple diamond) show the large difference between the results of Ref. 2 *vs*. Ref. 41. Overall, excluding the outlier of the ΔE_a for the BSCF k_O* from Ref. 2, a clear correlation is observed for both ΔE_as of the k_O* and D_O* *vs*. the calculated bulk O *2p*-band centers. The source of the large discrepancy between this correlation and the outlier activation barrier of k_O* of BSCF in Ref. 2 is not clear at present.

References

(1) Jacobson, A. J. Materials for Solid Oxide Fuel Cells. *Chemistry of Materials* **2009,** *22*, 660-674.
(2) Tarancon, A.; Burriel, M.; Santiso, J.; Skinner, S. J.; Kilner, J. A. Advances in Layered Oxide Cathodes for Intermediate Temperature Solid Oxide Fuel Cells. *J. Mater. Chem.* **2010,** *20*, 3799-3813.
(3) Tsipis, E. V.; Kharton, V. V. Electrode Materials and Reaction Mechanisms in Solid Oxide Fuel Cells: A Brief Review. *J. Solid State Electrochem.* **2008,** *12*, 1367-1391.
(4) Sun, C.; Hui, R.; Roller, J. Cathode Materials for Solid Oxide Fuel Cells: A Review. *J. Solid State Electrochem.* **2010,** *14*, 1125-1144.
(5) Claus, J.; Borchardt, G.; Weber, S.; Hiver, J.-M.; Scherrer, S. Combination of EBSP Measurements and SIMS to Study Crystallographic Orientation Dependence of Diffusivities in a Polycrystalline Material: Oxygen Tracer Diffusion in $La_{2-x}Sr_xCuO_{4\pm\delta}$. *Materials Science and Engineering: B* **1996,** *38*, 251-257.
(6) Tealdi, C.; Ferrara, C.; Mustarelli, P.; Islam, M. S. Vacancy and Interstitial Oxide Ion Migration in Heavily Doped $La_{2-x}Sr_xCoO_{4+/-\delta}$. *J. Mater. Chem.* **2012,** *22*, 8969-8975.
(7) Yashima, M.; Enoki, M.; Wakita, T.; Ali, R.; Matsushita, Y.; Izumi, F.; Ishihara, T. Structural Disorder and Diffusional Pathway of Oxide Ions in a Doped Pr_2NiO_4-Based Mixed Conductor. *Journal of the American Chemical Society* **2008,** *130*, 2762-2763.
(8) Parfitt, D.; Chroneos, A.; Kilner, J. A.; Grimes, R. W. Molecular Dynamics Study of Oxygen Diffusion in $Pr_2NiO_{4+\delta}$. *Physical Chemistry Chemical Physics* **2010,** *12*, 6834-6836.
(9) Chroneos, A.; Yildiz, B.; Tarancon, A.; Parfitt, D.; Kilner, J. A. Oxygen Diffusion in Solid Oxide Fuel Cell Cathode and Electrolyte Materials: Mechanistic Insights from Atomistic Simulations. *Energy & Environmental Science* **2011,** *4*, 2774-2789.
(10) Kushima, A.; Parfitt, D.; Chroneos, A.; Yildiz, B.; Kilner, J. A.; Grimes, R. W. Interstitialcy Diffusion of Oxygen in Tetragonal $La_2CoO_{4+\delta}$. *Physical Chemistry Chemical Physics* **2011,** *13*, 2242-2249.
(11) Bassat, J. M.; Odier, P.; Villesuzanne, A.; Marin, C.; Pouchard, M. Anisotropic Ionic Transport Properties in $La_2NiO_{4+\delta}$ Single Crystals. *Solid State Ionics* **2004,** *167*, 341-347.
(12) Burriel, M.; Garcia, G.; Santiso, J.; Kilner, J. A.; Richard, J. C. C.; Skinner, S. J. Anisotropic Oxygen Diffusion Properties in Epitaxial Thin Films of $La_2NiO_{4+\delta}$. *J. Mater. Chem.* **2008,** *18*, 416-422.
(13) Villesuzanne, A.; Paulus, W.; Cousson, A.; Hosoya, S.; Le Dréau, L.; Hernandez, O.; Prestipino, C.; Ikbel Houchati, M.; Schefer, J. On the Role of Lattice Dynamics on Low-Temperature Oxygen Mobility in Solid Oxides: A Neutron Diffraction and First-Principles Investigation of $La_2CuO_{4+\delta}$. *J. Solid State Electrochem.* **2011,** *15*, 357-366.
(14) Bassat, J.-M.; Burriel, M.; Wahyudi, O.; Castaing, R.; Ceretti, M.; Veber, P.; Weill, I.; Villesuzanne, A.; Grenier, J.-C.; Paulus, W.; Kilner, J. A. Anisotropic Oxygen Diffusion Properties in $Pr_2NiO_{4+\delta}$ and $Nd_2NiO_{4+\delta}$ Single Crystals. *The Journal of Physical Chemistry C* **2013,** *117*, 26466-26472.
(15) Perrichon, A.; Piovano, A.; Boehm, M.; Zbiri, M.; Johnson, M.; Schober, H.; Ceretti, M.; Paulus, W. Lattice Dynamics Modified by Excess Oxygen in $Nd_2NiO_{4+\delta}$: Triggering Low-Temperature Oxygen Diffusion. *The Journal of Physical Chemistry C* **2015,** *119*, 1557-1564.

(16) Routbort, J. L.; Rothman, S. J.; Flandermeyer, B. K.; Nowicki, L. J.; Baker, J. E. Oxygen Diffusion in $La_{2-x}Sr_xCuO_{4-y}$. *J. Mater. Res.* **1988,** *3*, 116-121.
(17) Skinner, S. J.; Kilner, J. A. A Comparison of The Transport Properties of $La_{2-x}Sr_xNi_{1-y}Fe_yO_{4+\delta}$ where $0 < x < 0.2$ and $0 < y < 0.2$. *Ionics* **1999,** *5*, 171-174.
(18) Boehm, E.; Bassat, J. M.; Dordor, P.; Mauvy, F.; Grenier, J. C.; Stevens, P. Oxygen Diffusion and Transport Properties in Non-Stoichiometric $Ln_{2-x}NiO_{4+\delta}$ Oxides. *Solid State Ionics* **2005,** *176*, 2717-2725.
(19) Opila, E. J.; Tuller, H. L.; Wuensch, B. J.; Maier, J. Oxygen Tracer Diffusion in $La_{2-x}Sr_xCuO_{4-y}$ Single Crystals. *Journal of the American Ceramic Society* **1993,** *76*, 2363-2369.
(20) Lee, D.; Lee, Y.-L.; Grimaud, A.; Hong, W. T.; Biegalski, M. D.; Morgan, D.; Shao-Horn, Y. Strontium influence on the oxygen electrocatalysis of $La_{2-x}Sr_xNiO_{4+/-\delta}$ ($0.0 \leq x_{Sr} \leq 1.0$) thin films. *Journal of Materials Chemistry A* **2014,** *2*, 6480-6487.
(21) Chen, Y.; Téllez, H.; Burriel, M.; Yang, F.; Tsvetkov, N.; Cai, Z.; McComb, D. W.; Kilner, J. A.; Yildiz, B. Segregated Chemistry and Structure on (001) and (100) Surfaces of $(La_{1-x}Sr_x)_2CoO_4$ Override the Crystal Anisotropy in Oxygen Exchange Kinetics. *Chemistry of Materials* **2015,** *27*, 5436-5450.
(22) Tomkiewicz, A. C.; Tamimi, M. A.; Huq, A.; McIntosh, S. Is the Surface Oxygen Exchange Rate Linked to Bulk Ion Diffusivity in Mixed Conducting Ruddlesden-Popper Phases? *Faraday Discussions* **2015,** *182*, 113-127.
(23) la O', G. J.; Ahn, S.-J.; Crumlin, E.; Orikasa, Y.; Biegalski, M. D.; Christen, H. M.; Shao-Horn, Y. Catalytic Activity Enhancement for Oxygen Reduction on Epitaxial Perovskite Thin Films for Solid-Oxide Fuel Cells. *Angewandte Chemie International Edition* **2010,** *49*, 5344–5347.
(24) Boehm, E.; Bassat, J. M.; Steil, M. C.; Dordor, P.; Mauvy, F.; Grenier, J. C. Oxygen Transport Properties of $La_2Ni_{1-x}Cu_xO_{4+\delta}$ Mixed Conducting Oxides. *Solid State Sci.* **2003,** *5*, 973-981.
(25) Boehm, E.; Bassat, J. M.; Dordor, P.; Mauvy, F.; Grenier, J. C.; Stevens, P. Oxygen Diffusion and Transport Properties in Non-Stoichiometric $Ln_{2-x}NiO_{4+\delta}$ Oxides. *Solid State Ionics* **2005,** *176*, 2717-2725.
(26) Munnings, C. N.; Skinner, S. J.; Amow, G.; Whitfield, P. S.; Davidson, I. J. Oxygen Transport in the $La_2Ni_{1-x}Co_xO_{4+\delta}$ System. *Solid State Ionics* **2005,** *176*, 1895-1901.
(27) Steele, B. C. H. Interfacial Reactions Associated with Ceramic Ion Transport Membranes. *Solid State Ionics* **1995,** *75*, 157-165.
(28) Bouwmeester, H. J. M.; Kruidhof, H.; Burggraaf, A. J. Importance of the Surface Exchange Kinetics as Rate Limiting Step in Oxygen Permeation Through Mixed-Conducting Oxides. *Solid State Ionics* **1994,** *72, Part 2*, 185-194.
(29) Baumann, F. S.; Fleig, J.; Habermeier, H.-U.; Maier, J. Impedance spectroscopic study on well-defined (La,Sr)(Co,Fe)$O_{3-\delta}$ model electrodes. *Solid State Ionics* **2006,** *177*, 1071-1081.
(30) Kreller, C. R.; McDonald, T. J.; Adler, S. B.; Crumlin, E. J.; Mutoro, E.; Ahn, S. J.; la O', G. J.; Shao-Horn, Y.; Biegalski, M. D.; Christen, H. M.; Chater, R. R.; Kilner, J. A. Origin of Enhanced Chemical Capacitance in $La_{0.8}Sr_{0.2}CoO_{3-\delta}$ Thin Film Electrodes. *Journal of The Electrochemical Society* **2013,** *160*, F931-F942.
(31) Takeda, Y.; Kanno, R.; Noda, M.; Tomida, Y.; Yamamoto, O. Cathodic Polarization Phenomena of Perovskite Oxide Electrodes with Stabilized Zirconia. *Journal of the Electrochemical Society* **1987,** *134*, 2656-2661.

(32) Escudero, M. J.; Aguadero, A.; Alonso, J. A.; Daza, L. A Kinetic Study of Oxygen Reduction Reaction on La_2NiO_4 Cathodes by Means of Impedance Spectroscopy. *Journal of Electroanalytical Chemistry* **2007,** *611*, 107-116.
(33) Lee, Y.-L.; Kleis, J.; Rossmeisl, J.; Shao-Horn, Y.; Morgan, D. Prediction of Solid Oxide Fuel Cell Cathode Activity with First-Principles Descriptors. *Energy & Environmental Science* **2011,** *4*, 3966-3970.
(34) Burriel, M.; Wilkins, S.; Hill, J. P.; Munoz-Marquez, M. A.; Brongersma, H. H.; Kilner, J. A.; Ryan, M. P.; Skinner, S. J. Absence of Ni on the Outer Surface of Sr Doped La_2NiO_4 Single Crystals. *Energy & Environmental Science* **2014,** *7*, 311-316.
(35) Lee, Y.-L.; Kleis, J.; Rossmeisl, J.; Morgan, D. *Ab Initio* Energetics of $LaBO_3$ (001) (B = Mn, Fe, Co, and Ni) for solid oxide fuel cell cathodes. *Physical Review B (Condensed Matter and Materials Physics)* **2009,** *80*, 224101.
(36) Read, M. S. D.; Islam, M. S.; Watson, G. W.; Hancock, F. E. Surface structures and defect properties of pure and doped La2NiO4. *J. Mater. Chem.* **2001,** *11*, 2597-2602.
(37) Han, J. W.; Yildiz, B. Mechanism for Enhanced Oxygen Reduction Kinetics at the $(La,Sr)CoO_{3-\delta}/(La,Sr)_2CoO_{4+\delta}$ Hetero-Interface. *Energy & Environmental Science* **2012,** *5*, 8598-8607.
(38) Sayers, R.; De Souza, R. A.; Kilner, J. A.; Skinner, S. J. Low Temperature Diffusion and Oxygen Stoichiometry in Lanthanum Nickelate. *Solid State Ionics* **2010,** *181*, 386-391.
(39) Feng, Z.; Yacoby, Y.; Gadre, M. J.; Lee, Y.-L.; Hong, W. T.; Zhou, H.; Biegalski, M. D.; Christen, H. M.; Adler, S. B.; Morgan, D.; Shao-Horn, Y. Anomalous Interface and Surface Strontium Segregation in $(La_{1-y}Sr_y)_2CoO_{4\pm\delta}/La_{1-x}Sr_xCoO_{3-\delta}$ Heterostructured Thin Films. *The Journal of Physical Chemistry Letters* **2014,** *5*, 1027-1034.
(40) Benson, S. J.; Chater, R. J.; Kilner, J. A. In *Proceedings of the Third International Symposium on Ionic and Mixed Conducting Ceramics*, The Third International Symposium on Ionic and Mixed Conducting Ceramics, Paris, France, Ramanarayanan, T. A., Ed. Electrochemical Society (1998): Paris, France, 1997; p 596.
(41) Bucher, E.; Egger, A.; Ried, P.; Sitte, W.; Holtappels, P. Oxygen Nonstoichiometry and Exchange Kinetics of $Ba_{0.5}Sr_{0.5}Co_{0.8}Fe_{0.2}O_{3-\delta}$. *Solid State Ionics* **2008,** *179*, 1032-1035.